Article

Mechanistic Insights into an Unprecedented C–C Bond Activation on a Rh/Ga Bimetallic Complex: A Combined Experimental/Computational Approach

Thomas Cadenbach, Christian Gemel, Rochus Schmid, and Roland A. Fischer

J. Am. Chem. Soc., **2005**, 127 (48), 17068-17078• DOI: 10.1021/ja055298d • Publication Date (Web): 10 November 2005

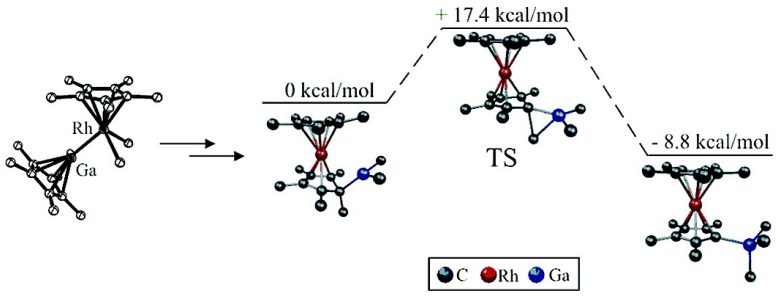

More About This Article

Additional resources and features associated with this article are available within the HTML version:

- Supporting Information
- Links to the 6 articles that cite this article, as of the time of this article download
- Access to high resolution figures
- Links to articles and content related to this article
- Copyright permission to reproduce figures and/or text from this article

View the Full Text HTML

J|A|C|S
ARTICLES
Published on Web 11/10/2005

Mechanistic Insights into an Unprecedented C−C Bond Activation on a Rh/Ga Bimetallic Complex: A Combined Experimental/Computational Approach

Thomas Cadenbach, Christian Gemel, Rochus Schmid, and Roland A. Fischer*

Contribution† from the Anorganische Chemie II, Organometallics & Materials, Ruhr-Universität Bochum, D-44780 Bochum, Germany

Received August 13, 2005; E-mail: roland.fischer@ruhr-uni-bochum.de

Abstract: The unusual rearrangement of [RhCp*(GaCp*)(CH_3)$_2$] (**1c**) to [RhCp*($C_5Me_4Ga(CH_3)_3$)] (**2**) is presented and its mechanism is discussed in detail. ^{13}C MAS NMR spectroscopy revealed that the title reaction proceeds cleanly not only in solution but also in solid state, which supports a unimolecular reaction pathway. On the basis of ^{1}H, ^{13}C, and ROESY NMR spectroscopy as well as isolation and structural elucidation of the hydrolysis product, the compound [RhCp*(*endo*-η^4-$C_5Me_5GaMe_2$)] (**3a**) was identified as a crucial reaction intermediate. DFT calculations on the B3LYP level of theory support this assignment and suggest a concerted C−C bond activation mechanism that topologically takes place at the gallium center. Furthermore, two fluxional processes of the reaction intermediate **3a** were studied experimentally as well as by computational methods. First, a mechanism takes place similar to a ring-slipping process that exchanges a $GaMe_2$ group between adjacent ring carbon atoms within the same Cp* ring. This process proceeds at a rate comparable to the NMR time scale and indeed is calculated to be energetically very favorable. Second, a unimolecular exchange process of the $GaMe_2$ group between the two Cp* rings of **3a** could be experimentally proven by the introduction of phenyl substituents as a label into the Cp* ligands at both sites, the rhodium as well as the gallium center. A series of experiments including deuteration studies and competition reactions was performed to substantiate the suggested mechanism being in accordance with DFT calculations on possible transition states.

Introduction

The coordination chemistry of carbenoid ligands of the heavier main group elements at transition metal centers has continued to be a major driving force in the development of fundamental organometallic chemistry since the early days of Fischer's discovery of the transition metal−carbon multiple bonds.[1] However, with the now very famous exception of the so-called N-heterocyclic carbenes, NHCs,[2−4] almost none of the various subclasses of transition metal carbenoid ligand complexes gained importance beyond the detailed understanding of their structure and bonding situations. Strictly speaking, serious examples for a potential *use* of carbenoid species of heavier main group elements as controlling ligands in transition-metal-mediated organic synthesis, as is the case for CO, phosphines, or NHCs, are—not surprisingly—virtually nonexistent. Namely, the coordination chemistry of silylenes[5−7] and borylenes[8−11] has been extensively studied aiming at the understanding of mechanistic aspects of catalytic transformations involving silylations and borylations mediated by transition-metal centers, but not in the view of tuning the reactivity of the transition-metal center itself. On the other hand, the recent report on the first triple bond between lead and a transition metal center, e.g. *trans*-[Br(PMe_3)$_4$Mo≡Pb(2,6-$C_6H_3R'_2$)] [R′ = (triisopropylphenyl)phenyl] may be regarded as a typical case of research primarily focusing on static aspects of structure and bonding only.[12] The same is largely true for the chemistry of ECp* (E = Al, Ga, In) and related low-valent group 13 metal compounds ER (R = $C(SiMe_3)_3$, bulky bis-imidinates, etc.) being formally isolobal to CO and/or cationic alkylidine fragments CR^+, the chemistry of which developed into its own field in the past decade.[13] For instance, we described novel homoleptic clusters [M_a(ECp*)$_b$], adopting solid-state structures similar to the classical carbonyl clusters [$M_a(CO)_b$] and thus going well beyond the coordination chemistry of other heavier carbenoid complexes.[14−17] In solution, the clusters [M_a(ECp*)$_b$] exhibit a rich fluxional behavior following *inter*- as well as *intra*molecular

† Organo group 13 complexes of transition metals XXXIX; for XXXVIII, see ref 17.

(1) Tokitoh, N.; Okazaki, R. *Coord. Chem. Rev.* **2000**, *210*, 251.
(2) Crabtree, R. H.; Peris, E. *Coord. Chem. Rev.* **2004**, *248*, 2239.
(3) Gade, L. H.; Stephane, B.-L.; Vincent, C. *Chem. Soc. Rev.* **2004**, *33*, 619.
(4) Hillier, A. C.; Grasa, G. A.; Viciu, M. S.; Lee, H. M.; Yang, C.; Nolan, S. P. *J. Organomet. Chem.* **2002**, *653*, 69.
(5) Brunner, H. *Angew. Chem., Int. Ed.* **2004**, *43*, 2749.
(6) Milstein, D.; Goikhman, R. *Chem. Eur. J.* **2005**, *11*, 2983.
(7) Tilley, T. D.; Glaser, P. B. *J. Am. Chem. Soc* **2003**, *125*, 13640.
(8) Braunschweig, H. *Angew. Chem., Int. Ed. Engl.* **1998**, *37*, 1786.
(9) Braunschweig, H.; Colling, M. *Coord. Chem. Rev.* **2001**, *223*, 1.
(10) Braunschweig, H.; Colling, M. *Eur. J. Inorg. Chem.* **2003**, 393.
(11) Braunschweig, H. *Adv. Organomet. Chem.* **2004**, *51*, 163.
(12) Filippou, A. C.; Rohde, H.; Schnakenburg, G. *Angew. Chem.* **2004**, *116*, 2293.
(13) Uhl, W.; Pohlmann, M.; Wartchow, R. *Angew. Chem.* **1998**, *110*, 1007.
(14) Steinke, T.; Gemel, C.; Winter, M.; Fischer, R. A. *Angew. Chem.* **2002**, *114*, 4955.
(15) Gemel, C.; Steinke, T.; Weiss, D.; Cokoja, M.; Winter, M.; Fischer, R. A. *Organometallics* **2003**, *22*, 2705.

10.1021/ja055298d CCC: $30.25

Scheme 1. Reaction of [RhCp*(GaCp*)$(CH_3)_2$] (**1c**) Giving [RhCp*$(C_5Me_4E(CH_3)_3)$] (**2**)

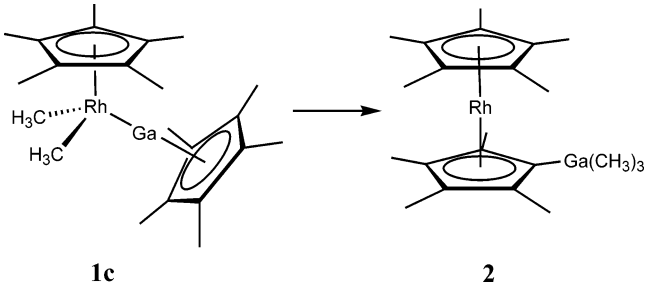

1c **2**

mechanisms of ligand exchange. In part, this exclusivity of ECp* ligands compared to other heavier main group carbenoids is based on their distinctive electronic characteristics. They combine exceptionally potent σ-donor and rather weak π-acceptor properties with the soft coordination behavior of Cp*, allowing haptotropic shifts and thus a delicate mediation of the steric and electronic situation at the group 13 center.[18−20] Only quite recently, coordinatively unsaturated intermediates such as [Ni(AlCp*)$_n$] ($n < 4$)[21] and [Fe(AlCp*)$_m$] ($m < 5$)[22] were found to activate C−H bonds under very mild conditions, i.e. aromatic C−H bonds by an *inter*molecular reaction in the former case and aliphatic C−H bonds by an *intra*molecular reaction in the latter case. On coordination of ECp*, the electron density of the transition metal is considerably increased, leaving at the same time an electrophilic group 13 metal center. Both the resulting nucleophilic, oxidizable, transition metal as well as the electrophilic main group metal represent the principal requirements for bond activation reactions. These findings point to the quite unique potential of these rather exotic species ECp* (or ER in general) to be considered as novel controlling ligands in organometallic chemistry.

In the course of these investigations we recently discovered an unprecedented C−C bond activation in the reaction of [RhCp*(L)$(CH_3)_2$] [L = DMSO (**1a**), pyridine (**1b**)] with GaCp* or AlCp*, giving the zwitterionic species [RhCp*$(C_5Me_4E(CH_3)_3)$] (**2**) (Scheme 1).[23] The stability of the 18 VE rhodenocenium structure together with the oxidation of Ga(I) to Ga(III) clearly represents a strong driving force. This complex rearrangement for E = Ga was shown to proceed via the substitution product [RhCp*(GaCp*)$(CH_3)_2$] (**1c**), which could be isolated and characterized. Complex **1c** was observed to be very labile also in the solid state, showing a color change from deep orange to pale brown within a few minutes at 60 °C. The solution NMR spectra of this pale residue were identical with the spectra of the final reaction product **2**, which was taken as the first indication that the reaction from **1c** to **2** also proceeds cleanly in the solid state.

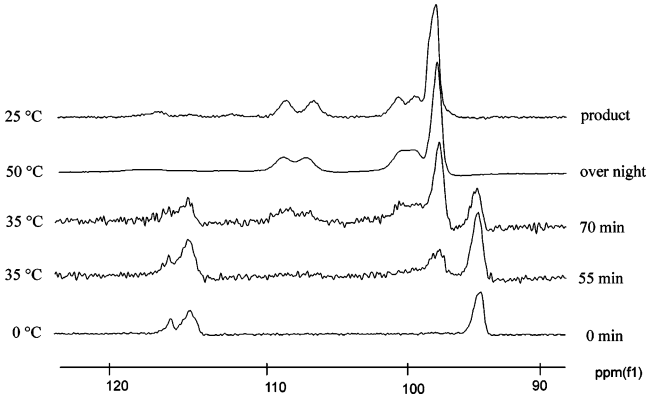

Figure 1. Representative cutout (85−130 ppm) of VT ^{13}C-MAS NMR spectra of the solid-state reaction of **1c** giving **2**.

The moderate reaction rates matching the NMR time scale combined with the synthetic accessibility of potential intermediates and the rather unusual possibility to directly compare the reaction in the solid state with the solution prompted us to look in detail into the mechanism of the title reaction in order to learn more about the *reactive* aspects of carbenoid group 13 ligands attached to a transition-metal center. Our investigations are based on a thorough experimental analysis of a crucial intermediate by means of 1D and 2D NMR spectroscopic techniques, isotope labeling studies, cross-mixing experiments, as well as theoretical modeling of the whole reaction sequence searching for possible transition states, intermediates, and alternative mechanisms on the B3LYP[24,25]/LanL2DZ[26] level of theory.[27]

Results and Discussion

Reaction in the Solid State. To verify that the reaction of **1c** to **2** does indeed proceed not only in solution but also in the solid state, a series of ^{13}C MAS NMR spectra of **1c** was recorded. Figure 1 illustrates a representative cutout of spectra obtained as a subject to temperature and time (a figure containing the full spectra is available in the Supporting Information). Evidently, the formation of **2** proceeds cleanly also in the solid state, however, without the spectroscopic appearance of intermediates.

The most important consequence from this observation is the fact that at least one *inter*molecular pathway connecting **1c** with **2** must be energetically available, not ruling out competing alternatives in solution. Foremost, evidence of such an *intra*molecular pathway validates efforts to support the experiments by a computational approach, as likely mechanistic alternatives are more strongly limited and thus much easier to model than would be in the case of distinctly *inter*molecular mechanisms.

Reaction in Solution. Monitoring the reaction from **1c** to **2** by ^{1}H NMR shows a strong dependence of the resulting spectra on the solvent used. We found, that in the presence of donors, such as pyridine or THF, an intermediate (**3**) appears, which subsequently disappears in due course of the reaction, finally leading to a clean ^{1}H NMR spectrum of **2** under all conditions.

(16) Steinke, T.; Gemel, C.; Winter, M.; Fischer, R. A. *Chem. Eur. J.* **2005**, *11*, 1636.
(17) Buchin, B.; Gemel, C.; Cadenbach, T.; Fischer, R. A. *Inorg. Chem.* **2005**, *44*, submitted.
(18) Steinke, T.; Gemel, C.; Cokoja, M.; Fischer, R. A. *J. Chem. Soc., Dalton Trans.* **2005**, 55.
(19) Cokoja, M.; Gemel, C.; Steinke, T.; Schroeder, F.; Fischer, R. A. *J. Chem. Soc., Dalton Trans.* **2005**, 44.
(20) Steinke, T.; Gemel, C.; Cokoja, M.; Winter, M.; Fischer, R. A. *Chem. Commun.* **2003**, 1066.
(21) Steinke, T.; Gemel, C.; Cokoja, M.; Winter, M.; Fischer, R. A. *Angew. Chem.* **2004**, *116*, 2349.
(22) Steinke, T.; Cokoja, M.; Gemel, C.; Kempter, A.; Krapp, A.; Frenking, G.; Zenneck, U.; Fischer, R. A. *Angew. Chem.* **2005**, *117*, 3003.
(23) Cadenbach, T.; Gemel, C.; Schmid, R.; Block, S.; Fischer, R. A. *J. Chem. Soc., Dalton Trans.* **2004**, 3171.
(24) Becke, A. D. *J. Chem. Phys.* **1993**, *98*, 5648.
(25) Parr, R. G.; Yang, W.; Lee, C. *Phys. Rev. B* **1988**, *37*, 785.
(26) Dunning, T. H.; Hay, P. J. *Modern Theoretical Chemistry*, Plenum: New York, 1976; Vol. 3.
(27) All energies in this paper are given as relative free energies $\Delta G°$ for the standard state. For comparison the zero-point energy corrected E_{DFT} values are given in the Figures 3, 4, and 6 in brackets.

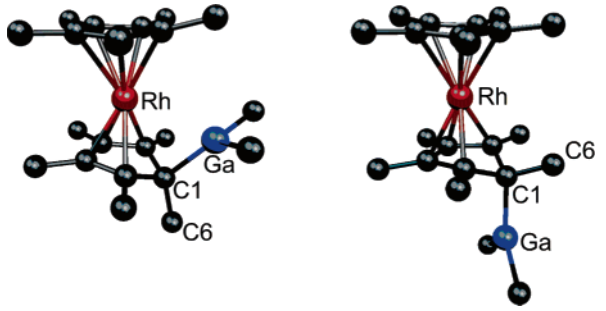

Figure 2. Possible intermediates **3a** and **3b**.

The ^{1}H NMR spectrum of **3** consists of three singlets in an integral ratio of 15:15:6, representing two chemically nonequivalent Cp* rings and two chemically equivalent CH_3 groups. Noticeable, one of the Cp* signals is considerably broadened, suggesting that some kind of fluxional behavior is involved. Indeed, at −40 °C this broad signal splits into three sharp singlets in an integral ratio of 6:6:3. The fluxional process becomes slower with increasing donor strength of the solvent [$w_{1/2}(C_6D_6/1$ equiv py) = 9.23 Hz; $w_{1/2}$(py) = 34.6 Hz], and at the same time the stability of **3** increases. In neat pyridine, for example, **3** is stable at room temperature for at least 5 days. Only heating the solution above 40 °C for 1 h allows detection of **2**.

The fact that the signal for the two CH_3 groups initially bound to the rhodium atom does not show a Rh−CH_3 coupling clearly suggests that both methyl groups have migrated from the rhodium to the gallium center. Additionally, the presence of two signals each representing 15 protons points to the fact that both Cp* ligands are still intact, i.e. no C−C activation has taken place at this point of the reaction. Further insight into the molecular structure of **3** is gained by analysis of the low-temperature ^{13}C NMR spectrum: At −100 °C the ^{13}C NMR spectrum in THF shows five doublets at 90.1 (J_{RhC} = 5.48 Hz), 83.8 (J_{RhC} = 9.10 Hz), 62.3 (J_{RhC} = 13.17 Hz), 56.9 (J_{RhC} = 6.85 Hz), and 29.3 ppm (J_{RhC} = 4.53 Hz), as well as four singlets at 11.5, 9.7, 8.3, and −3.9 ppm. The doublet at 90.1 ppm integrating to approximately five carbons can unequivocally be assigned to the aromatic carbon atoms of the RhCp* moiety. The presence of two more doublets in the olefinic region, each integrating to two carbon atoms, indicates a structure where direct Rh−C bonds are established also to the second Cp* ring. η^4-Coordination of the diene moiety of (η^1-Cp*)$GaMe_2$ to the RhCp* fragment forming an 18 VE Rh(I) complex is a reasonable suggestion for the molecular structure of **3** and consistent with the NMR spectra. The signals at 83.8 and 62.3 ppm can be assigned to the internal and the terminal carbon atoms of the diene moiety, respectively. The four singlets in the aliphatic region of the ^{13}C NMR spectrum subsequently belong to the methyl groups of the Rh(C_5*Me*$_5$) moiety (5C, 8.3 ppm), the C_5*Me*$_4$(Me)$GaMe_2$ unit (2C, 11.5 ppm and 2C, 9.7 ppm), and the Ga*Me*$_2$ group (2C, −3.9 ppm). Consequently, the sp^3 carbon of the Cp*$GaMe_2$ fragment (C1) and its adjacent methyl group (C6) give rise to the remaining two doublets at 56.9 and 29.3 ppm.

Two stereoisomers of this intermediate are possible: (i) a structure where the $GaMe_2$ unit is located in an endo-position with respect to the RhCp* moiety (**3a**) and (ii) a structure with an exo-orientation of the $GaMe_2$ unit (**3b**). Figure 2 illustrates the calculated optimized structures fore these two isomers.

The fact that C1 and as well C6 show a rather large Rh−C coupling (J_{RhC} = 6.85 and 4.53 Hz, respectively) cannot be explained at this point. An agostic interaction of the C−CH_3 bond and the rhodium center, for example (which could be the case for structure **3b**), is ruled out due to the formal 18 VE count of the transition metal. However, the question whether **3a** or **3b** corresponds to the actually spectroscopically observed species cannot be decided solely on the basis of the ^{13}C NMR spectrum.

Mechanistic Hypotheses for the Reaction of 1 to 2. In principle, three different pathways for the reaction of **1c** to **2** are feasible with either the endo-complex **3a** or the exo-complex **3b** as a reaction intermediate (Scheme 2). In all three mechanisms the first step is a transfer of a single methyl group from the rhodium to the gallium center, giving the spectroscopically nondetectable intermediate "Rh(II)−Ga(II)" species **4**. The transfer of the second methyl group from the rhodium to the gallium under coordination of the diene moiety of the Cp*$GaMe_2$ formed yields either **3a** (pathway A) or **3b** (pathways B and C) as the consecutive reaction intermediates.

In pathway A, the actual C−C bond rupture takes place at the gallium center of **3a** via a direct transfer of the exo-oriented methyl group (C6) to the endo-oriented $GaMe_2$ moiety. Pathway B describes a similar mechanism, with the exception that the locations of the migrating CH_3 group and the $GaMe_2$ moiety are now swapped, i.e. the endo-oriented CH_3 (C6) group in **3b** is directly transferred to the exo-oriented $GaMe_2$ moiety via a concerted mechanism. Pathway C takes into account that the endo-oriented CH_3 group in **3b** can first migrate to the rhodium center (i.e. a "classic" C−C bond activation at a Rh(I) center),[28,29] giving the half-sandwich Rh(III) complex **5**, bearing a methyl group and a σ-bound ($C_5Me_4GaMe_2$) ligand. Subsequent transfer of the methyl group to the gallium and coordination of the resulting ($C_5Me_4GaMe_3$) unit to the rhodium center finally lead to the formation of **2**. The question if **3a** or **3b** is the experimentally observed intermediate must be addressed experimentally. However, to compare all three pathways with respect to the energies of their intermediates and transition states, also DFT calculations were performed.

Characterization of the Key Intermediate 3a/b. Several attempts to crystallize the intermediate **3a/b** failed due to its high solubility under the conditions of formation and stabilization. We followed two major strategies for an adequate stereochemical analysis of **3a/b**: (i) a reasonable chemical modification of the intermediate in order to sufficiently suppress the bond activation step and thus to obtain an X-ray single-crystal structure of the modified intermediate and (ii) 2D ROESY NMR spectroscopy.

In an attempt to chemically modify **3a/b**, a freshly prepared solution of this intermediate in THF was treated with an equimolar amount of salicylic acid with the intent to hydrolyze the sterically accessible Ga−CH_3 groups under formation of a chelating gallium salicylate complex. However, monitoring this reaction by ^{1}H NMR spectroscopy shows that both Ga−CH_3 bonds remain intact and instead the hydrolysis of the Cp*-Ga bond takes place, forming [Cp*Rh(C_5Me_5H)] (**6**) and [(salicylate)$GaMe_2$] as the reaction products. **6** is also obtained by

(28) Crabtree, R. H.; Dion, R. P.; Gibboni, D. J.; McGrath, R. B.; Holt, M. S. *J. Am. Chem. Soc.* **1986**, *108*, 7222.
(29) Crabtree, R. H.; Dion, R. P. *Chem. Commun.* **1984**, 1260.

Scheme 2. Mechanistic Working Hypotheses for the Intramolecular Rearrangement of **1c** into **2**

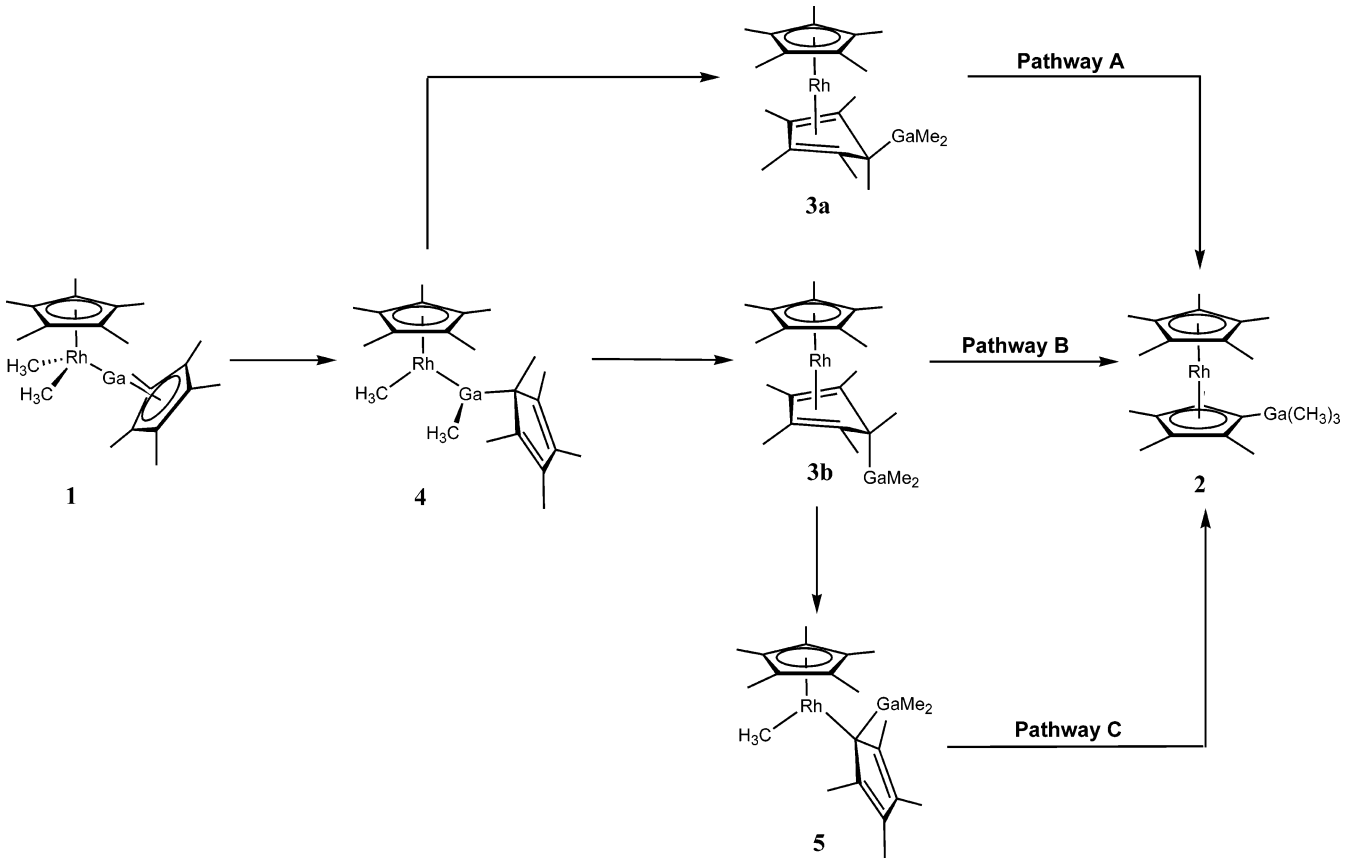

hydrolysis with an excess of acetic acid, whereas HCl/Et_2O or H_2O lead to complete decomposition of the material. **6** can be obtained analytically pure in high yields by sublimation of the crude product in vacuo as well-shaped yellow single crystals.

An X-ray crystal structure of **6** (Figure 5) reveals the methyl group C6 to be located in the exo-position with respect to the RhCp* fragment. It should be mentioned that the respective endo-isomer of this compound has been electrochemically prepared and analyzed by ^{1}H NMR spectroscopy.[30]

Since the mechanism of the hydrolysis reaction and particularly its stereochemical consequences are unclear, the exo-orientation of the methyl group in **6** is not necessarily an indication for an endo-orientation of the $GaMe_2$ group in **3**. However, the ^{13}C NMR spectrum of **6** reveals a strong spectroscopic similarity to **3a/b** (Table 1).

Above all, C1 as well as the C6 exhibit large Rh−C coupling constants in both complexes. At this point the origin of this unusually strong $^2J_{RhC}$ and $^3J_{RhC}$ coupling is uncertain; probably the nearly ideal zigzag geometry in the bonding arrangement of the rhodium atom, the *exo*-methyl group, and the two linking C5 ring carbon atoms is responsible for the strong magnetic communication between the nuclei. Thus, the C1−C6 axis in the solid-state structure of **6** is almost perfectly perpendicular to the diene plane of the C_5Me_5H ligand (87.5°) and hence almost perfectly parallel to the Rh−diene$_{centroid}$ axis. Noteworthy, the endo-oriented proton in **6** does not show a detectable J_{RhH} coupling. However, the strong similarity of the ^{13}C NMR spectra of **3a/b** and **6** is an indication of, yet not convincing evidence for the presence of **3a**.

(30) Gusev, O. V.; Denisovich, L. I.; Peterleitner, M. G.; Rubezhov, A. Z.; Ustynyuk, N. A.; Maitlis, P. M. *J. Organomet. Chem.* **1993**, *452*, 219.

To collect further experimental support for the endo-structure **3a** as the key intermediate of the title reaction, a 2D ROESY spectrum was recorded. The minimum H−H distance of the RhCp* and the $GaMe_2$ fragments in the minimized structure of **3a** is 2.38 Å, and therefore, a cross-peak between these two signals is expected in the case of an endo-orientation of the $GaMe_2$ fragment. In the case of **3b**, no such signal should be observed. Indeed, the appearance of a strong ROESY cross-peak for the RhCp* and the $GaMe_2$ signals unequivocally points to **3a**.

DFT Calculations for Pathways A, B, and C. Figure 3 depicts the calculated pathways for the formation of **3a** and **3b** from **1c**. The formation of the "Rh(II)−Ga(II)" intermediate **4** resulting from **1c** via migration of one CH_3 group from the rhodium to the gallium center is calculated to be endergonic by 7.9 kcal/mol. This cost in energy is partially a result of a change in the coordination mode of the GaCp* ring, shifting from η^5 in **1c** to η^1 in **4**. The energy of the transition state of this process (**TS1**) is 11.3 kcal/mol above that of **1c** and also points to the loss of aromatization energy of the GaCp* ring.

The next step in the reaction is the migration of the second Rh−CH_3 group to the gallium center under simultaneous η^4-coordination of the diene moiety of the [(η^1-C_5Me_5)($GaMe_2$)] fragment to the rhodium atom. In the case of **3a**, i.e. an endo-arrangement of the $GaMe_2$ group with respect to the RhCp* fragment, a transition state (**TS2a**) could be located, being only 2.8 kcal/mol above **4** (which is 10.7 kcal/mol above **1c**).

In contrast to the formation of **3a**, no transition state could be located for the direct conversion of **4** to **3b** (**TS2b**). It is questionable if such a direct conversion is possible at all, since a 180° rotation of the [C_5Me_5($GaMe_2$)] moiety perpendicular

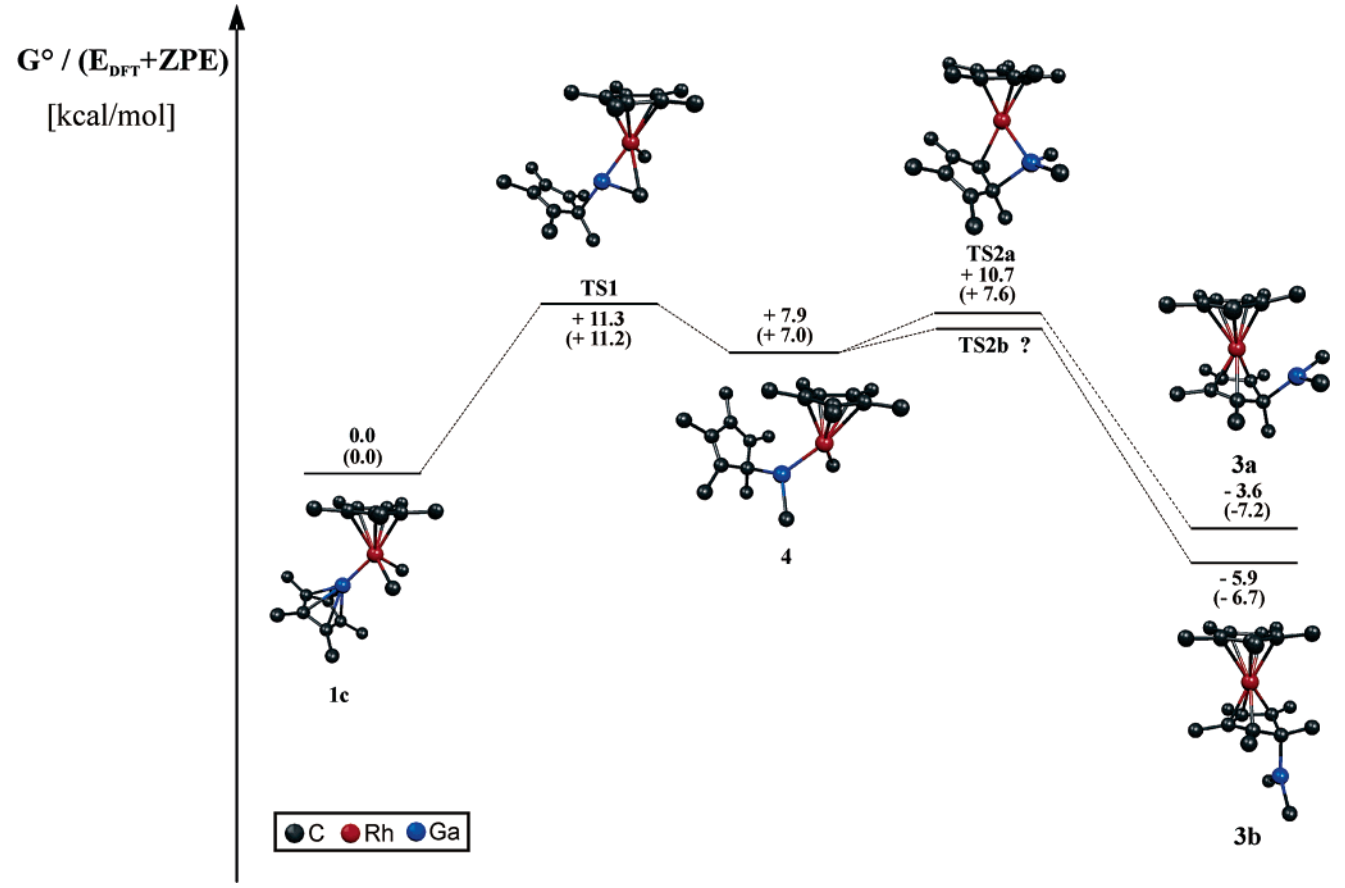

Figure 3. Calculated pathway for the formation of **3a** and **3b** from **1c**.

to its bond axis to the rhodium center is needed, a movement that seems to be impossible without prior dissociation of the whole fragment. Such a dissociative process, however, is expected to be energetically very unfavorable and does, above all, not cope with a unimolecular rearrangement sequence for the conversion of **1c** to **2**. Even so, a unimolecular conversion from **4** to **3b** can certainly not be ruled out solely on the basis of its transition state not being located computationally. Thermodynamically **3b** is more favorable than **3a** by 2.3 kcal/mol, which is apparently a consequence of the steric interference of the $GaMe_2$ group with the RhCp* fragment in **3a** (smallest H−H distance = 2.38 Å). When comparing the energies of the pyridine adducts of **3a** and **3b**, this difference becomes even more evident, now being 7.5 kcal/mol. The stronger interaction of the pyridine with the acidic gallium in **3b** is well-reflected by its significantly smaller Ga−N bond length (Ga−N = 2.13 Å in **3b** vs 2.19 Å in **3a**).

Figure 4 illustrates pathways A, B, and C for the C−C activation process. The final reaction product **2** is calculated to be more stable than the starting complex **1c** by 12.4 kcal/mol. It should be noted here that the geometrical features of the optimized structures of both **1c** and **2** are in good agreement with the X-ray crystal structures (see Supporting Information for further information).

The transition state **TS3A** for the rearrangement of **3a** to **2** could be located and is energetically 17.4 kcal/mol above **3a**. This is a remarkably small activation barrier for a C−C bond rupture and thus is in good agreement with the experimentally observed fact that the reaction of **1c** to **2** is taking place under exceptionally mild reaction conditions in solution as well as in the solid state. The reaction is a concerted migration of the CH_3 group (C6), with **TS3A** exhibiting a classical five-coordinate carbon "halfway" between the C5 ring and the gallium center. On a closer look at the bond lengths of **TS3A** and comparison with the respective structural features of **1c** and **2**, it becomes apparent that the migration of the gallium atom toward the methyl group proceeds concomitantly with an elongation of the C−C bond. This movement of the gallium in the direction of the C5 ring plane of the product allows an interaction of C1 with the rhodium center, i.e. a partial aromatization of the C5 ring already in the stage of **TS3A**, which is probably responsible for the low activation barrier.

The transition state **TS3B** for pathway B, starting out from the exo-isomer **3b**, is energetically by far more unfavorable than **TS3A**, being 33.2 kcal/mol above **3b**. The geometrical reaction characteristics for pathways A and B are in general very similar, where **TS3B** is also representing a "classical" transition state for a concerted bond activation process. However, as the positions of the $GaMe_2$ group and the CH_3 group (C6) are now swapped with respect to pathway A, an interaction of C1 with the rhodium atom in **TS3B** is sterically impossible. This missing interaction, which is also reflected by the higher distortion of the C5 ring from planarity in **TS3B**, evidently accounts for its relatively high energy.

For the third pathway (pathway C) the intermediate **5** as well as the respective transition state **TS3C** could be optimized on the potential energy surface. **5** is energetically less favorable than **3b** by 19.3 kcal/mol. **TS3C** is unexpectedly high in energy, being 56.9 kcal/mol above **3b**. This is a surprising result, since C−C activation barriers on Rh(I) centers are typically consider-

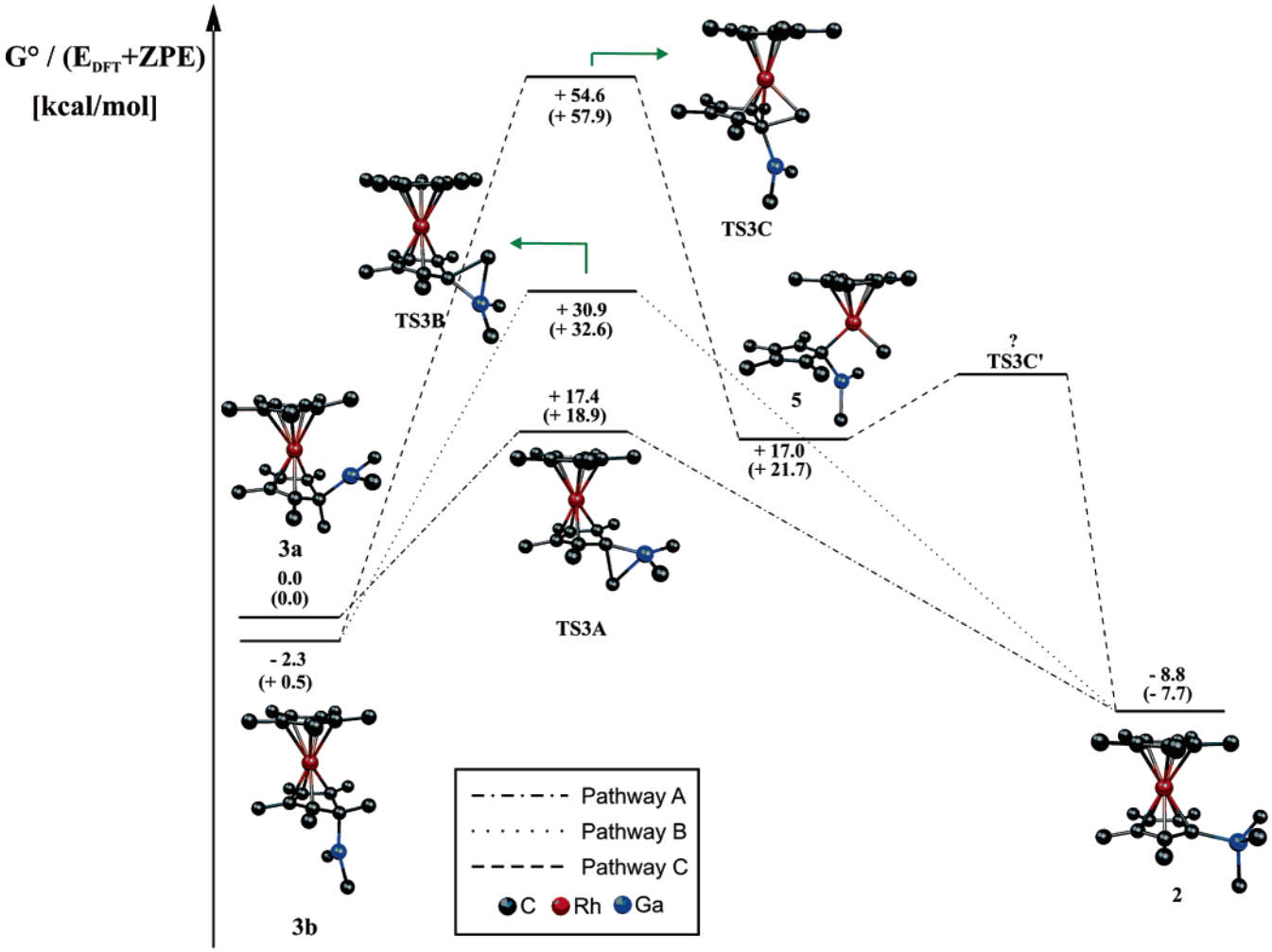

Figure 4. Calculated pathways A, B and C for the C−C bond-breaking step.

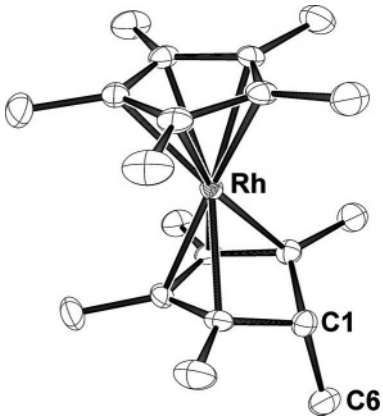

Figure 5. Structure of the hydrolysis product **6** of **3a** in the solid state.

Table 1. Comparison of Chemical Shifts and Coupling Constants J_{RhC} of **3a/b** and **6**

	3a/b	6
δ(C1), ppm	56.9	61.5
δ(C6), ppm	29.3	24.2
$^2J_{RhC}$(C1), Hz	6.85	5.34
$^3J_{RhC}$(C6), Hz	4.53	3.47

ably lower.[31] The transition state for the final methyl group migration in pathway C (**TS3C′**) could not be located despite several attempts. However, the low energies of **TS1** and **TS2a** suggest that the methyl group migration from the rhodium to the gallium atom should not be the limiting step for pathway C.

Several important conclusions can be gained from these computations: **3a** as well as **3b** clearly represent likely intermediates in the reaction of **1c** to **2**. Isomer **3b** is thermodynamically more stable than **3a**, particularly when stabilized by pyridine, which is present in the actual reaction system. Yet, no direct path from **1c** to **3b** could be found. In addition, the barrier for the C−C activation is very low for **3a** but considerably higher for both pathways involving **3b**. This is in very good agreement with the experimental facts suggesting **3a** as the important reaction intermediate (vide supra).

Fluxional Processes of 3a. On the basis of the structure of **3a**, two possible fluxional processes become evident (Scheme 3): First, a ring-slipping process of the Ga(C_5Me_5)Me_2 ligand, best described as a "spinning" movement of the $GaMe_2$ fragment around the Rh−Cp*$_{centroid}$ axis (fluctuation A). This movement is presumably responsible for the experimentally observed coalescence of the Cp* methyl groups. Second, it is conceivable that a Cp* ring-exchange process takes place, i.e. a movement where the direct Ga−C bond to one Cp* ring is broken and subsequently a new Ga−C bond to the second Cp* ring is formed (fluctuation B). No evidence for this process is gained

(31) Rybtchinski, B.; Milstein, D. *Angew. Chem.* **1999**, *111*, 918.

Scheme 3. Possible Fluxional Processes of **3a**

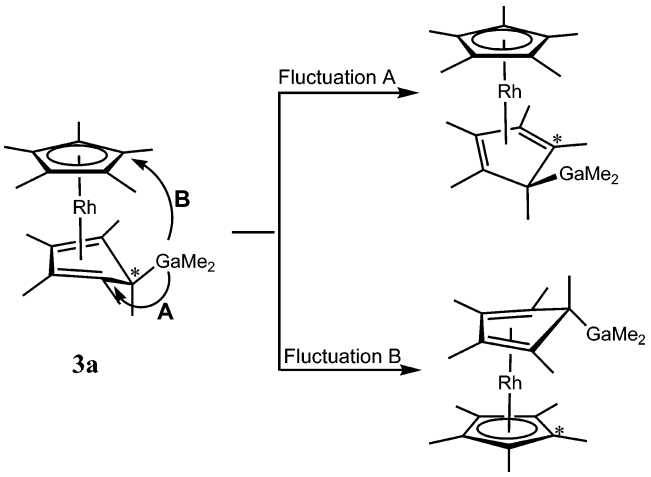

from the ^{1}H or ^{13}C NMR spectra of **3a**, which either means that it is slower than the NMR time scale or nonexistent at all. However, experimental evidence of a unimolecular mechanism for fluctuation B would be a strong proof for **3a** as the reaction intermediate. Thus, both processes were studied experimentally by spectroscopic and synthetic techniques, as well as by computational modeling of the reactions' pathways.

The activation energy for fluctuation A could be experimentally determined by low-temperature NMR spectroscopy. ^{1}H NMR spectra were measured at −33, −25, −14, −3, and 13 °C and the line widths of the resulting spectra compared to fitted spectra resulting from simulations. By a thus obtained Eyring plot ($R^2 = 0.98$) the activation energy is calculated to be 22.6 kcal/mol. This value is considerably higher than the energy of the respective calculated transition state (**TS4**). However, it must be taken into account that the rate was determined in a solution containing a comparably high concentration of pyridine, which stabilizes **3a/b** under the conditions of our experiments (vide supra). Thus, the actual concentration of **3a** in solution is certainly decreased in a dissociation/association equilibrium with the pyridine complex, which itself is not expected to undergo a similar fluxional process. The fact that both high concentrations of pyridine and very low temperatures retard the fluxional processes substantiates this assumption.

Thus, it seemed impossible to gain spectroscopic evidence for the slower process, i.e. fluctuation B. Broadening of the ^{1}H NMR line width of the RhCp* signal never observed, no matter what conditions we tried. For that reason, no further NMR studies such as ECSY or DANTE experiments were performed; instead a labeling approach for the elucidation of process B was given preference.

The introduction of one phenyl group instead of one methyl group in one of the two Cp* rings in **1c** allows us to chemically and spectroscopically distinguish between the two Cp* rings. This results in either [Rh(C_5Me_4Ph)(GaCp*)Me_2] (**9**), if the phenyl group is attached to the RhCp* fragment, or [Rh(Cp*)-(GaC_5Me_4Ph)Me_2] (**10**), if the phenyl group is introduced into the GaCp* moiety. **9** could be isolated and spectroscopically characterized, whereas **10** can be prepared only in situ due to its high reactivity. According to ^{1}H NMR, starting from both compounds, a mixture of two products is formed: [Rh(C_5Me_4-Ph)($C_5Me_4PhGaMe_3$)] (**11a**), a complex where the $GaMe_3$ and the phenyl group are attached to two different rings, and [RhCp*($C_5Me_3PhGaMe_3$)] (**11b**), where both groups are attached to the same ring. Interestingly, the molar ratio of these two isomers is identical, being 80 (**11a**) to 20 (**11b**) for both reactions!

The aliphatic region of the ^{1}H NMR spectrum of **11a** consists of five singlets at 1.79 (6H), 1.49 (6H), 1.43 (6H), 1.02 (6H), and 0.20 ppm (9H). The aliphatic part of the ^{1}H NMR spectrum of the minor isomer **11b** also consists of five peaks, however, showing different integral ratios. The signal at 1.35 ppm (15H) can be easily assigned to the RhCp* fragment and the signal at 0.22 ppm to the $GaMe_3$ group. The ring methyl groups of the [$C_5Me_3Ph(GaMe_3)$] moiety give rise to three signals at 1.98, 1.933, and 1.932 ppm, all integrating to three protons. On the basis of these spectral data it cannot be unequivocally decided if either the ortho- or meta-isomer of **11b**, respectively, is formed. The assigned chemical shifts for **11a** and **11b** were cross-checked by isolation and spectroscopic characterization of [Rh(C_5Me_4Ph)($C_5Me_3PhGaMe_3$)] (**12**), which can be obtained by reaction of [Rh(C_5Me_4Ph)(pyridine)Me_2] (**12**) and Ga-(C_5Me_4Ph). Single crystals of the major isomer **11a** were obtained by crystallization from THF/Et_2O. The solid-state structure does not show any unexpected geometric features, and a representation of the molecular structure can be obtained from the Supporting Information.

The fact that the same ratio of **11a** and **11b** are obtained by starting from either **9** or **10** can be regarded as experimental evidence for fluctuation B, however, only if a unimolecular mechanism is assumed. An experimental indication for this can be gained from the solid-state reaction of **9**. Thus, a crystalline sample of **9** was heated to 60 °C for 1 min, leading to a color change from orange red to pale brown. Indeed, the ^{1}H NMR spectrum in C_6D_6 of the solid obtained consists of exactly the same signals in the same ratios as the ^{1}H NMR spectra obtained from the solution reactions of **9** and **10**.

The calculated energetic minima and transition states responsible for both fluxional processes in **3a** are depicted in Figure

Scheme 4. Reaction of Complexes of the Type **1c** Labeled with One Phenyl Group

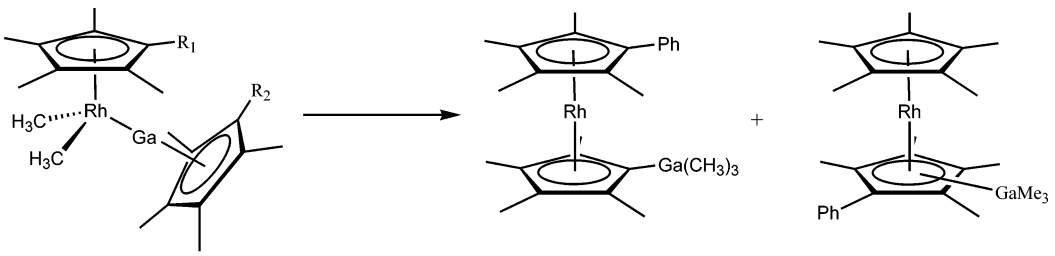

R_1 = Ph, R_2 = Me **(9)**
R_1 = Me, R_2 = Ph **(10)**

11a **11b**

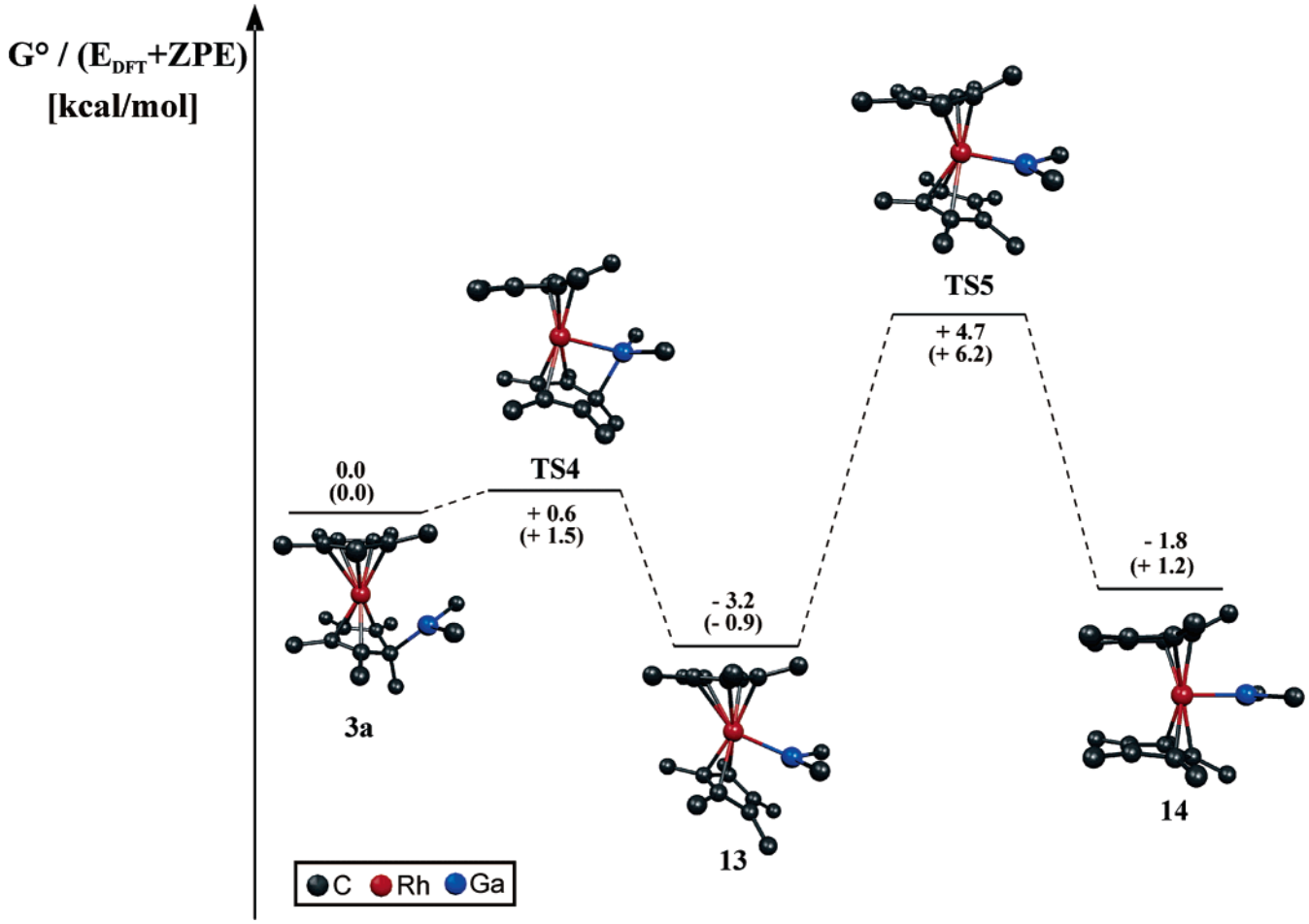

Figure 6. Calculated minima and transition states for the fluctional processes of **3a**.

6. Complexes **13** and **14** both represent isomers of **3a**, in which no strong Ga−Cp* bond exists, but rather a direct Rh−$GaMe_2$ bond is formed. Both are energetic minima that are geometrically very similar to each other and basically differ in the exact position of the $GaMe_2$ group as well as the position of one of the two Cp* rings. Species **14** represents a C_{2v} symmetric molecule; i.e. the rhodium, the gallium and the two carbons bound to the gallium are exactly coplanar, constructing a mirror plane for the two Cp* rings. Thus, it can be considered as the key intermediate for fluctuation B. In **13** this C_{2v} symmetry is broken by a slight movement of the $GaMe_2$ fragment toward one Cp* ring [Ga−C1 = 2.63 Å (**7**), 3.03 Å (**8**)]. **13** is lower in energy than **14** by 1.4 kcal/mol, which itself is more stable in energy than **3a** by 1.8 kcal/mol.

No direct pathway from **3a** to **14** was found, instead two transition states could be localized between **3a** and **13** (**TS4**) and between **13** and **14** (**TS5**), respectively. **TS4** is energetically extremely low (0.6 kcal/mol above **3a**). In contrast, the transition state for the reaction of **13** to **14** (**TS5**) is calculated to be astonishingly high, being 7.9 kcal/mol above **13**, although **13** and **14** are structurally very similar. However, this is well consistent with the fact that fluctuation A is spectroscopically observed, while fluctuation B is not.

All experimental as well as computational results presented so far suggest **3a** as the reaction intermediate and thus pathway A (Scheme 2) as the reaction mechanism. This is strongly based on the fact that the solid-state reactions of **1c** to **2** (or from **9** to **11a/b**, respectively) can be taken as experimental evidence for a favorable unimolecular reaction pathway. However, the solid-state reaction does not exclude competing bimolecular mechanisms working in solution! Indeed, a simple cross-mixing ^1H NMR experiment proves the existence of such a mechanism of exchanging CH_3 groups between two complexes. Thus, a solution of the selectively deuterated complex [RhCp*(GaCp*)-$(CD_3)_2$] (**1cD**[6]) and the nondeuterated phenyl-marked complex [Rh(C_5Me_4Ph)(GaCp*)Me_2] (**9**) (1:1 ratio) in C_6D_6 was heated to 60 °C for 45 min. As expected, the product mixture consists of the three compounds **2**, **11a**, and **11b**. As evident from the integral ratios of the three $GaMe_3$ signals at 0.17 (**2**), 0.20 (**11a**), and 0.22 ppm (**11b**), a statistic distribution of the CD_3 groups to all three products occurs. The same result is obtained if two solutions of the respective intermediates analogous to **3a** are prepared independently and subsequently mixed and heated to induce the activation reaction. This means that either methyl groups are exchanged between two gallium centers of **3a** (e.g. via Ga−CH_3−Ga bridges) or $GaMe_2$ groups are exchanged between two complexes of **3a**. An exchange of whole (C_5Me_4-$GaMe_2$) units should be energetically the most unfavorable, since dissociation of the strongly bound diene moiety from the Rh^I center is necessary. Furthermore, in the reactions of **9** and **10**, no traces of either **2** or **12** were observed, which should be expected if the whole diene fragments are exchanged between complexes. However, experimentally it is hard to finally prove whether such a diene exchange reaction takes place at all. Preliminary DFT calculations do not exclude the dissociation of $[GaMe_2]^+$ ions (stabilized by pyridine) from **3a** under

formation of the anion $[Rh(Cp^*)_2]^-$, although the energy for this process is calculated to be rather high (26.3 kcal/mol; calculated in THF as the solvent, with the PCM method).[32−35] At this point, the nature of the exchange process in solution cannot be further elucidated; more detailed DFT calculations are needed and are the subject of current research.

Conclusions

The thermal rearrangement of $[Cp^*Rh(GaCp^*)(CH_3)_2]$ (**1c**) proceeds under very mild condition in solution as well as in the solid state, giving the zwitterionic species $[RhCp^*(C_5Me_4)(GaMe_3)]$ (**2**) as the final product. As an intermediate, the Rh(I) species $[RhCp^*(\eta^4\text{-}C_5Me_5GaMe_2]$ (**3a**) could be spectroscopically identified, with 2D ROESY spectroscopy pointing to an endo-arrangement of the $GaMe_2$ moiety with respect to the RhCp* fragment. DFT calculations strongly support these experimental results, indicating that **3a** indeed represents an energetic minimum at reasonable energy. The C−C activation step from **3a** giving **2** is calculated to have a very low activation barrier (17.4 kcal/mol), which is well-reflected by the mild experimental conditions for the overall reaction. In contrast, alternative mechanisms involving the exo-isomer **3b** were calculated to have considerably higher activation barriers. The crucial reaction intermediate **3a** is shown to undergo two fluxional processes: (i) migration of the $GaMe_2$ group from one Cp* ring carbon atom to an adjacent one (fluctuation A) and (ii) the migration of the $GaMe_2$ group from one Cp* ligand to the second one (fluctuation B). Both processes could be calculated to proceed via the same intermediates. In solution, both *intra*molecular as well as *inter*molecular processes seem to be activated as evidenced from labeling studies and cross-mixing experiments. The *inter*molecular mechanisms could be neither experimentally proven nor computationally understood, which is basically a result of their expected complexity.

What is finally achieved by this mechanistic study? As stated above, the major part of the transition-metal chemistry of low-valent main-group metal ligands has been focused on structural and theoretical issues. Aspects such as the abilities of carbenoid metalloid ligands to tune the reactivity of transition-metal centers have not been addressed before in detail. The title reaction provided us with a model for a detailed study of the cooperative effects originating from the proximity or coordination of a potentially very electrophilic gallium center to a very nucleophilic d^8 rhodium(I) center (as in **3a**) or to a more electrophilic d^6 rhodium(III) center (as in **1c**) and its consequences for typical organometallic reactions: migrations of alkyl groups to coordinated electrophilic ligands and C−C bond splitting. The carbenoid character as well as the electrophilicity of the GaCp* ligand in the starting complex provokes a reduction of the Rh(III) to a reactive Rh(I) center in the course of the alkyl migration, at the same time creating a very Lewis acidic $[(\eta^1\text{-}C_5Me_5)Ga(Me)_2]$ moiety. This oxidized Ga(III) center represents the actual reaction site for a C−C bond splitting process with a surprisingly small activation barrier, the electrons for this process evidently coming from the nucleophilic Rh(I) center. Altogether, the course of the reaction is clearly determined by both metal centers effectively cooperating in a redox cascade creating intermediates with exceptionally reactive metal centers in close proximity to each other and opening a number of low activation energy pathways. The question of how to capitalize on this rather fascinating and complex situation in catalytic or stoichiometric processes has still to be addressed. Admittedly, the group-13 carbenoid and metalloid ligands of the general type ER are still quite exotic. However, GaCp* and its congeners may represent model cases of strong donor ligands not being innocent spectators such as phosphanes or NHCs but taking active part in specific reactions, thus representing an intermediate state between ancillary ligands and cooperative metal centers. Apart from this more traditional point of view, such complexes may also be considered as molecular models for the surface reactivity of intermetallic materials such as transition-metal aluminides, gallides, and indides, being potentially relevant for heterogeneous catalysis. Since it is known that AlCp* can stabilize molecular clusters such as $[Al_{38}(AlCp^*)_{12}]$[36] or $[Ni_8(AlCp^*)_6]$,[37] the mechanistic study presented herein may at least stimulate thinking about the reactivity of such metal-rich compounds or related nanoparticles.

Experimental Section

General Remarks. All manipulations were carried out in an atmosphere of purified argon using standard Schlenk and glovebox techniques. Hexane, toluene, THF, and Et_2O were dried using an mBraun solvent purification system, all other solvents were dried by distillation over standard drying agents. The final H_2O content in all solvents used was checked by Karl Fischer titration and did not exceed 5 ppm. $[(RhCp^*Cl_2)_2]$,[38] GaCp*,[39] C_5Me_4PhH,[40] $Ga(C_5Me_4Ph)$,[41] $Zn(CD_3)_2$,[42] and $[Cp^*Rh(DMSO)(CH_3)_2]$ (**1a**)[23] were prepared according to literature methods. Elemental analyses were performed by the Microanalytical Laboratory of the University of Essen. NMR spectra were recorded on a Bruker Avance DPX-250 spectrometer (^1H, 250.1 MHz; ^{13}C, 62.9 MHz) at 298 K unless otherwise stated. Chemical shifts are given relative to TMS and were referenced to the solvent resonances as internal standards.

The crystal structures of **6** and **13a** were measured on a Oxford Excalibur 2 diffractometer using Mo Kα radiation ($\lambda = 0.710\,73$ Å). The structures were solved by direct methods using SHELXS-97 and refined against F^2 on all data by full-matrix least-squares with SHELXL-97 (SHELX-97 program package, Sheldrick, Universität Göttingen 1997).

CCDC-288415 (**6**) and CCDC-288416 (**13a**) contain the supplementary crystallographic data for this paper. These data can be obtained free of charge via www.ccdc.cam.ac.uk/conts/retrieving.html (or from the Cambridge Crystallographic Data Center, 12 Union Road, Cambridge CB21EZ, UK; fax: (+44)1223−336−033; deposit@ccdc.cam.uk).

Computational Details. All calculations were performed with the Gaussian98 (rev. A11) program package.[43] DFT calculations were carried out using the hybrid exchange-correlation functional B3LYP[24,25] together with the Los Alamos National Laboratory double-ζ LanL2DZ basis set.[26] All structures were fully optimized without symmetry

(32) Barone, V.; Scalmani, G.; Rega, N.; Cossi, M. *J. Chem. Phys.* **2001**, *114*, 5691.
(33) Barone, V.; Rega, N.; Scalmani, G.; Cossi, M. *J. Chem. Phys.* **2002**, *117*, 43.
(34) Tomasi, J.; Cancés, E.; Mennucci, B. *J. Phys. Chem. B* **1997**, *101*, 10506.
(35) Tomasi, J.; Mennucci, B.; Cancés, E. *J. Chem. Phys.* **1997**, *107*, 3032.
(36) Vollet, J.; Hartig, J. R.; Schnöckel, H. *Angew. Chem.* **2004**, *116*, 3248.
(37) Steinke, T.; Gemel, C.; Fischer, R. A. *Angew. Chem.* **2005**, *117*, to be submitted.
(38) Wang, J. W.; Moseley, K.; Maitlis, P. M. *J. Am. Chem. Soc.* **1969**, *91*, 5970.
(39) Jutzi, P.; Schebaum, L. O. *J. Organomet. Chem.* **2002**, *654*, 176.
(40) Bjoergvinsson, M.; Halldorsson, S.; Arnason, I.; Magull, J.; Fenske, D. *J. Organomet. Chem.* **1997**, *544*, 207.
(41) Buchin, B.; Steinke, T.; Gemel, C.; Cadenbach, T.; Fischer, R. A. *Z. Anorg. Allg. Chem.* **2005**, in press.
(42) Petrier, C.; Souza Barbosa, J. C. d.; Dupuy, C.; Luche, J. L. *J. Org. Chem.* **1985**, *50*, 5761.
(43) Frisch, M. J.; et al. *Gaussian 98*, Revision A.11; Gaussian, Inc.: Pittsburgh, PA, 2001.

Table 2. Basis Set Comparison for the Calculation of Two Key Steps of the Reaction Sequence

	LanL2DZ	6-311G**(C, H, Ga)/ Stuttgart RSC 1997 ECP (Rh)
3a	0	0
3b	+0.5	+1.0
TS3A	+18.9	+21.3
TS3C	+57.9	+64.7
5	+21.7	+29.8
2	−7.7	−7.7

constraints. Vibrational frequencies were calculated for all stationary points to ensure that local minima were located and to confirm that transition states had only one imaginary frequency. These vibrations were visually inspected using the MOLDEN program.[44] Transition states were located by means of the QST2 or QST3 approach, with an initial guess for the transition state gained from manipulation of the geometries of either the educts or the products, also using the MOLDEN software.

To verify that the overall qualitative mechanistic picture is not affected by the choice of the comparably small LanL2DZ basis set, single point calculations for two key steps (**3a/TS1A/2** and **3a/TS3C/5**) were performed using a significantly larger basis set (6-311G** [45,46] for C, H, Ga and Stuttgart RSC 1997 ECP[47] for Rh). The results (Table 2) indicate that the qualitative trends in energies and activation barriers are reasonably well reproduced by the LanL2DZ basis set.

Syntheses. [RhCp*(pyridine)Me$_2$] (1b). [{Cp*RhCl$_2$}$_2$] (1.03 g, 1.66 mmol) in 15 mL of THF was treated with pyridine (2.7 mL, 33.4 mmol) at room temperature. After stirring for 30 min, ZnMe$_2$ (2.4 mL of a 2.0 M solution in toluene, Aldrich; 4.80 mmol) was added at −80 °C to the orange suspension. The mixture was warmed to room temperature and stirred for 30 min, whereupon an orange solution formed. After hydrolysis by addition of H_2O (0.35 mL, 19.2 mmol), all volatiles were removed in vacuo, and the residue was extracted with toluene (3 × 5 mL doped with pyridine) at 0 °C. After removal of the solvent in vacuo, the residue was then extracted with *n*-hexane (3 × 5 mL) at 0 °C. The solvent volume was reduced to ca. 8 mL and cooled to −40 °C for 16 h to give the product as pale orange crystals. The crystals were isolated by means of canullation, washed with a small amount of cold *n*-hexane, and dried in vacuo. Yield: 0.89 g of orange crystals (77%). ^{1}H NMR δ_H (298 K, 250.1 MHz, C_6D_6): 8.21 (d, 2H), 6.69 (t, 1H), 6.29 (t, 2H), 1.55 (s, 15H), 0.75 (d, 6H, $^3J_{RhH}$ = 2.5 Hz); ^{13}C NMR δ_C (298 K, 62.9 MHz, C_6D_6): 154.5 (s), 134.7 (s), 124.3 (s), 92.3 (d, J_{RhC} = 4.8 Hz), 9.0 (s), 3.6 (d, J_{RhC} = 31.9 Hz). Anal. Calcd for ($C_{17}H_{26}$NRh): C, 58.79; H, 7.55; N, 4.03. Found: C, 58.01; H, 7.46; N, 4.0.

[RhCp*(GaCp*)Me$_2$] (1c). (RhCp*(pyridine)(CH$_3$)$_2$] (0.282 g, 0.812 mmol) was dissolved in toluene (8 mL), and GaCp* (0.183 g, 0.893 mmol) was added at 0 °C. Immediately, the color changed from orange to red. After stirring the solution for a further 10 min at 0 °C, the solvent was removed in vacuo and the residue extracted quickly with *n*-hexane (3 × 5 mL) at 0 °C. The solvent volume was reduced to ca. 5 mL and cooled to −40 °C for 16 h to give the product as light red crystals. The crystals were isolated by means of canullation, washed with a small amount of cold *n*-hexane, and dried in vacuo. Yield: 0.197 g of light red crystals (51%). ^{1}H NMR δ_H (298 K, 250.1 MHz, C_6D_6): 1.89 (s, 15H), 1.77 (s, 15H), 0.50 (d, 6H, $^3J_{RhH}$ = 2.7 Hz); ^{13}C NMR δ_C (298 K, 62.9 MHz, C_6D_6): 113.8 (s), 95.1 (d, J_{RhC} = 4.5 Hz), 10.4 (s), 9.7 (s), −14.3 (d, J_{RhC} = 26.8 Hz). Anal. Calcd for ($C_{22}H_{36}$GaRh): C, 55.85; H, 7.67. Found: C, 55.29; H, 7.58.

[RhCp*(pyridine)(CD$_3$)$_2$] (1bD^6). A suspension of CD_3I (1.450 g, 10 mmol), $ZnBr_2$ (1.115 g, 5 mmol), and Li wire (0.140 mg, 20 mmol) in a mixture of toluene (20 mL) and THF (3 mL) was sonicated at 0 °C for 5 h. The black suspension was filtered at −80 °C to a freshly prepared solution of [RhCp*(pyridine)Cl$_2$] (1.553 g, 4 mmol) in THF. The mixture was warmed to room temperature and stirred for 30 min, whereupon an orange solution formed. After hydrolysis (3.6 mL of H_2O, 0.2 mol) all volatiles were removed in vacuo, and the residue was extracted with toluene (3 × 10 mL doped with pyridine) at 0 °C. After removal of the solvent in vacuo, the residue was then extracted with *n*-hexane (3 × 15 mL) at 0 °C. The solvent volume was reduced to ca. 10 mL and cooled at −40 °C for 16 h to give the product as orange crystals. The crystals were isolated by means of canullation, washed with a small amount of cold *n*-hexane, and dried in vacuo. Yield: 1.11 g of orange crystals (80%). ^{1}H NMR δ_H (C_6D_6, 250 MHz, 25 °C): 8.19 (d, 2H), 6.68 (t, 1H), 6.27 (t, 2H), 1.56 (s, 15H); ^{13}C NMR δ_C (298 K, 62.9 MHz, C_6D_6): 154.3 (s), 134.6 (s), 124.1 (s), 92.1 (d, J_{RhC} = 4.7 Hz), 8.8 (s), 2.6 (br). Anal. Calcd for ($C_{17}H_{20}D_6$-NRh): C, 57.79; H, 9.13; N, 3.96. Found: C, 57.54; H, 8.10; N, 3.88.

[RhCp*(GaCp*)(CD$_3$)$_2$] (1cD^6). 1bD^6 (0.300 g, 0.864 mmol) was dissolved in toluene (7 mL) and GaCp* (0.212 g, 1.037 mmol) was added at 0 °C. Immediately, the color changed from orange to red. After stirring the solution for a further 10 min at 0 °C, the solvent was removed in vacuo and the residue fast-extracted with *n*-hexane (3 × 7 mL) at 0 °C. The solvent volume was reduced to ca. 5 mL and cooled to −40 °C for 16 h to give the product as light red crystals. The crystals were isolated by means of canullation, washed with a small amount of cold *n*-hexane, and dried in vacuo. Yield: 0.270 g of light red crystals (66%). ^{1}H NMR δ_H (173 K, 250.1 MHz, THF-d_8): 2.07 (s, 15H), 1.70 (s, 15H). ^{13}C NMR δ_C (173 K, 62.9 MHz, THF-d_8): 114.1 (s), 95.1 (d, J_{RhC} = 4.3 Hz), 10.5 (s), 9.97 (s), −14.7 (br). Anal. Calcd for ($C_{22}H_{30}D_6$GaRh): C, 55.14; H, 8.83. Found: C, 55.62; H, 7.92.

[RhCp*(C$_5$Me$_4$GaMe$_3$)] (2). Method A. [Cp*Rh(DMSO)(CH$_3$)$_2$] (**1a**) (0.150 g, 0.433 mmol) was dissolved in toluene (8 mL), and GaCp* (0.102 g, 0.498 mmol) was added. The solution was warmed to 60 °C and stirred for 1 h, whereupon a white precipitate was formed. After removal of all volatiles in vacuo, the residue was washed with hexane (3 × 5 mL) and dried in vacuo. The precipitate was redissolved in toluene (ca. 4 mL) and crystallized by slow evaporation of the solvent. Yield: 0.141 g of white crystals (69%). ^{1}H NMR δ_H (298 K, 250.1 MHz, C_6D_6): 1.77 (s, 6H), 1.34 (s, 15H), 1.06 (s, 6H), 0.15 (s, 9H); ^{13}C NMR δ_C (298 K, 62.9 MHz, C_6D_6): 117.8 (br), 106.8 (d, J_{RhC} = 8.5 Hz), 98.5 (d, J_{RhC} = 7.9 Hz), 96.5 (d, J_{RhC} = 7.3 Hz), 12.2 (s), 8.9 (s), 8.5 (s), 1.6 (s), −2.7 (s). Anal. Calcd ($C_{22}H_{36}$GaRh): C, 55.85; H, 7.67. Found: C, 55.14; H, 7.29.

Method B (Solid State). A crystalline sample of **1c** was heated to 60 °C for 2−3 min, whereupon a color change from red to pale brown was observed. The thus obtained product was analyzed by means of solution ^{1}H and ^{13}C NMR as well as ^{13}C MAS NMR. All spectroscopic data were identical with those of the product obtained by method A.

[RhCp*(C$_5$Me$_5$GaMe$_2$)] (3a). [Cp*Rh(GaCp*)(CH$_3$)$_2$] (0.043 g, 0.0906 mmol) was dissolved in pyridine-d^5 (1 mL) and stirred for 45 min at 25 °C. The thus obtained solution of **3a** was directly used for analysis without further workup. ^{1}H NMR δ_H (THF-d_8, 250 MHz, −100 °C): 1.77 (s, 15H), 1.76 (s, 6H), 0.50 (s, 6H), −0.04 (s, 3H), −0.16 (s, 6H); ^{13}C NMR δ_C (THF-d_8, 62.9 MHz, −100 °C): 90.9 (d, J_{RhC} = 5.48 Hz), 83.8 (d, J_{RhC} = 9.10 Hz), 62.3 (d, J_{RhC} = 13.17 Hz), 56.9 (d, J_{RhC} = 6.85 Hz), 29.3 (d, J_{RhC} = 4.53 Hz), 11.5 (s), 9.7 (s), 8.3 (s), −3.9 (s).

[RhCp*(C$_5$Me$_5$H)] (6). [Cp*Rh(GaCp*)(CH$_3$)$_2$] (0.700 g, 1.479 mmol) was dissolved in pyridine (10 mL) and stirred at 25 °C. After 45 min, acetic acid was added (0.266 g 4.437 mmol) and the reaction mixture was stirred for a further 5 min, whereupon a yellow solution and a white precipitate was formed. After removal of all volatiles in vacuo, the residue was extracted with hexane (3 × 5 mL). The solvent was removed in vacuo and the yellow residue sublimed at 50 °C in

(44) Schaftenaar, G.; Noordik, J. H. *J. Comput.-Aided Mol. Des.* **2000**, *14*, 123−134.
(45) Pople, J. A. *J. Chem. Phys.* **1980**, *72*, 650.
(46) Curtiss, L. A.; McGrath, M. P.; Blaudeau, J.-P.; Davis, N. E.; Binning, R. C., Jr.; Radom, L. *J. Chem. Phys.* **1995**, *103*, 6104.
(47) Dolg, M.; Wedig, U.; Stoll, H.; Preuss, H. *J. Chem. Phys.* **1987**, *86*, 866.

vacuo. Yield: 0.305 g (55%). ^{1}H NMR δ_H (298 K, 250.1 MHz, C_6D_6): 2.53 (q, 1H, J_{CH} = 6.08 Hz), 1.75 (s, 6H), 1.74 (s, 15H), 1.21 (s, 6H), 0.56 (d, 3H, J_{CH} = 6.06 Hz); ^{13}C NMR δ_C (298 K, 62.9 MHz, C_6D_6): 95.1 (d, J_{RhC} = 5.64 Hz), 88.4 (d, J_{RhC} = 9.58 Hz), 61.5 (d, J_{RhC} = 5.34 Hz), 59.8 (d, J_{RhC} = 13.06 Hz), 24.2 (d, J_{RhC} = 3.47 Hz), 15.1 (s),13.5 (s), 12.5 (s), 4.1 (s). Anal. Calcd for ($C_{20}H_{31}Rh$): C, 64.17; H, 8.35. Found: C, 65.15; H, 8.15.

[Rh(C$_5$Me$_4$Ph)Cl$_2$]$_2$ (7). A mixture of $RhCl_3 \cdot 3H_2O$ (5. g, 0.019 mol) and C_5Me_4HPh (3.76 g, 0.019 mol) in 40 mL of methanol was refluxed under nitrogen with stirring for 48 h. After the reaction mixture was cooled, the shiny red crystals were isolated by means of canullation, washed with a small amount of methanol, and dried in vacuo. Yield: 5.01 g (71%). ^{1}H NMR δ_H (THF-d_8, 250 MHz, 25 °C): 7.73 (m, 4H), 7.35 (m, 6H), 1.66 (s, 12H), 1.63 (s, 12H); ^{13}C NMR δ_C (C_6D_6, 62.9 MHz, 25 °C): 131.5 (s), 130.2 (s), 129.3 (s), 129.1 (s), 100.9 (d, J_{RhC} = 8.4 Hz), 93.8, (d, J_{RhC} = 7.5 Hz), 90.4 (d, J_{RhC} = 9.7 Hz), 10.7 (s), 9.6 (s). Anal. Calcd for ($C_{30}H_{34}Cl_4Rh_2$): C, 48.55, H, 4.62. Found: C, 48.40; H, 4.26.

[Rh(C$_5$Me$_4$Ph)(pyridine)Me$_2$] (8). Compound **9** (1.0 g, 1.35 mmol) in 15 mL of THF was treated with pyridine (2.7 mL, 33.4 mmol) at room temperature. After stirring for 30 min, $ZnMe_2$ (1.96 mL of a 2.0 M solution in toluene, Aldrich; 3.92 mmol) was added at −80 °C to the orange suspension. The mixture was warmed to room temperature and stirred for 30 min, whereupon a pale orange solution formed. After hydrolysis (0.35 mL H_2O, 19.6 mmol) all volatiles were removed in vacuo, and the residue was extracted with toluene (3 × 8 mL) at 0 °C. After removal of the solvent in vacuo, the residue was then extracted with *n*-hexane (3 × 10 mL) at 0 °C. The solvent volume was reduced to ca. 7 mL and cooled to −40 °C for 16 h to give the product as yellow crystals. The crystals were isolated by means of canullation, washed with a small amount of cold *n*-hexane, and dried in vacuo. Yield: 0.88 g (80%). ^{1}H NMR δ_H (C_6D_6, 250 MHz, 25 °C): 8.18 (d, 2H), 7.18 (m, 5H), 6.59 (t, 1H), 6.18 (t, 2H), 1.67 (s, 15H), 1.59 (s, 15H), 0.88 (d, 6H, $^3J_{RhH}$ = 2.5 Hz); ^{13}C NMR δ_C (C_6D_6, 62.9 MHz, 25 °C): 154.3 (s), 136.6 (s), 134.7 (s), 130.6 (s), 128.2 (s), 125.8 (s), 124.1 (s), 98.8 (d, J_{RhC} = 3.8 Hz), 98.5 (d, J_{RhC} = 4.1 Hz), 88.9 (d, J_{RhC} = 5.5 Hz), 9.9 (s), 8.7 (s), 4.6 (d, J_{RhC} = 31.5 Hz). Anal. Calcd for ($C_{22}H_{28}NRh$): C, 64.55; H, 6.89; N, 3.42. Found: C, 64.28; H, 6.79; N, 3.36.

[Rh(C$_5$Me$_4$Ph)(GaCp*)Me$_2$] (9). Compound **8** (0.5 g, 0.934 mmol) was dissolved in toluene (8 mL) and GaCp* (0.305 g, 1.50 mmol) was added at 25 °C. Immediately, the color changed from yellow to red. After stirring the solution for further 3 min at 25 °C, the solvent was removed in vacuo at 0 °C and the residue fast-extracted with *n*-hexane (3 × 7 mL) at 0 °C. The solvent volume was reduced to ca. 5 mL and cooled to −40 °C for 16 h to give the product as red crystals. The crystals were isolated by means of canullation, washed with a small amount of cold *n*-hexane, and dried in vacuo. Yield: 0.464 g (71%). ^{1}H NMR δ_H (C_6D_6, 250 MHz, 25 °C): 7.51 (m, 2H), 7.17 (m, 3H), 1.91 (s, 6H), 1.82 (s, 15H), 1.61 (s, 6H), 0.61 (d, 6H, $^3J_{RhH}$ = 2.63 Hz); ^{13}C NMR δ_C (THF-d_8, 62.9 MHz, −100 °C): 137.6 (s), 132.8 (s), 128.4 (s), 127.1 (s), 113.9 (s), 102.1 (d, J_{RhC} = 2.6 Hz), 99.6 (d, J_{RhC} = 1.8 Hz), 92.4 (d, J_{RhC} = 4.6 Hz), 12.1 (s), 9.8 (s), 8.1 (s), −13.4 (d, J_{RhC} = 26.8 Hz). Anal. Calcd for ($C_{27}H_{38}GaRh$): C, 60.59; H, 7.16. Found: C, 58.96; H, 6.45.

[Rh(C$_5$Me$_4$Ph)(C$_5$Me$_4$GaMe$_3$)] (11a) and [RhCp*(C$_5$Me$_3$PhGaMe$_3$)] (11b). Method A. Compound **8** (0.400 g, 0.977 mmol) was dissolved in toluene (8 mL), and GaCp* (0.260 g, 1.270 mmol) was added. The solution was warmed to 60 °C and stirred for 1 h, whereupon a white precipitate was formed. After removal of all volatiles in vacuo, the residue was washed with hexane (3 × 7 mL) and dried in vacuo. The residue was redissolved in THF and precipitated by slow diffusion of Et_2O to give the product as colorless crystals. Yield: 0.392 g (75%). ^{1}H NMR δ_H (C_6D_6, 250 MHz, 25 °C) [Rh(C_5Me_4Ph)($C_5Me_4GaMe_3$)], **11a**: 7.30 (m, 5H) 1.79 (s, 6H), 1.49 (s, 6H), 1.43 (s, 6H), 1.02 (s, 6H), 0.20 (s, 9H). ^{1}H NMR δ_H (C_6D_6, 250 MHz, 25 °C) [RhCp*-($C_5Me_3PhGaMe_3$)], **11b**: 7.30 (m, 5H) 1.98 (s, 3H), 1.93 (s, 3H), 1.93 (s, 3H), 1.35 (s, 15H), 0.22 (s, 9H); ^{13}C NMR δ_C (298 K, 62.9 MHz, C_6D_6) 130.8 (s), 130.6 (s), 107.3 (d, J_{RhC} = 8.3 Hz), 99.7 (d, J_{RhC} = 7.4 Hz), 99.1 (d, J_{RhC} = 7.6 Hz), 98.3 (d, J_{RhC} = 7.2 Hz), 97.3 (d, J_{RhC} = 7.3 Hz), 96.0 (d, J_{RhC} = 7.1 Hz), 12.3 (s), 9.8 (s), 8.9 (s), 8.4 (s), −3.0 (s). Anal. Calcd for ($C_{27}H_{38}GaRh$): C, 60.59; H, 7.16. Found: C, 59.31; H, 6.74.

Method B. Compound **1b** (0.282 g, 0.812 mmol) was dissolved in toluene (8 mL) and [Ga(C_5Me_4Ph)] (0.325 g, 1.218 mmol) was added. The solution was warmed to 60 °C and stirred for 1 h, whereupon a white precipitate was formed. After removal of all volatiles in vacuo, the residue was washed with hexane (3 × 5 mL) and dried in vacuo. Yield: 0.304 g (70%). All spectroscopic data were identical with those of the product obtained by method A.

Method C (Solid State). A crystalline sample of **9** was heated to 60 °C for 2−3 min, whereupon a color change from red to pale brown was observed. The thus obtained product was analyzed by means of solution ^{1}H and ^{13}C NMR as well as ^{13}C MAS NMR. All spectroscopic data were identical with those of the product obtained by methods A and B.

[Rh(C$_5$Me$_4$Ph)(C$_5$Me$_3$PhGaMe$_3$)] (12). Compound **8** (0.300 g, 0.733 mmol) was dissolved in toluene (8 mL), and [Ga(C_5Me_4Ph)] (0.254 g, 0.953 mmol) was added. The solution was warmed to 60 °C and stirred for 45 min, whereupon a pale brown precipitate formed. After removal of all volatiles in vacuo, the residue was washed with hexane (3 × 8 mL) and dried in vacuo. Yield: 0.333 g (76%). ^{1}H NMR δ_H (298 K, 250.1 MHz, C_6D_6): 7.10 (m, 10H), 2.04 (s, 3H), 1.85 (s, 3H), 1.63 (s, 3H), 1.61 (s, 3H), 1.46 (s, 6H), 1.26 (s, 3H), 0.21 (s, 9H); ^{13}C NMR δ_C (C_6D_6, 62.9 MHz, 25 °C): 131.4 (s), 130.9 (s), 130.7 (s), 130.6 (s), 128.8 (s), 128.5 (s), 128.0 (s), 119.7 (d, J_{RhC} = 6.7 Hz), 107.9 (d, J_{RhC} = 8.2 Hz), 107.5 (d, J_{RhC} = 8.1 Hz), 107.3 (d, J_{RhC} = 8.0 Hz), 104.6 (d, J_{RhC} = 7.4 Hz), 99.2 (d, J_{RhC} = 7.5 Hz), 99.1 (d, J_{RhC} = 7.4 Hz), 98.1 (d, J_{RhC} = 7.3 Hz), 97.4 (d, J_{RhC} = 7.1 Hz), 96.4 (d, J_{RhC} = 7.2 Hz), 13.9 (s), 12.6 (s), 10.4 (s), 10.1 (s), 9.94 (s), 9.90 (s), 9.2 (s), −2.5 (s). Anal. Calcd for ($C_{32}H_{40}GaRh$): C, 64.35; H, 6.75. Found: C, 63.57; H, 7.23.

Acknowledgment. We thank Gregor Barchan and Martin Gartmann for performing the 2D NMR experiments as well as Jochen Hauswald for his help in recording ^{13}C-MAS and VT-NMR spectra.

Supporting Information Available: Copies of NMR spectra (solution and solid state), crystal structure of **11a**, Eyring plot for fluctuation A, and comparison of computed and measured bond lengths and angles of **1c** and **2**, as well as Cartesian coordinates and energies of all structures (minima and TS) presented in this paper (PDF). This material is available free of charge via the Internet at http://pubs.acs.org.

JA055298D